Journal of Alloys and Compounds 660 (2016) 402–406

Contents lists available at ScienceDirect

Journal of Alloys and Compounds

journal homepage: http://www.elsevier.com/locate/jalcom

Structure, thermal analysis and dehydriding kinetic properties of $Na_{1-x}Li_xMgH_3$ hydrides

Zhong-min Wang*, Jia-jun Li, Song Tao, Jian-qiu Deng, Huaiying Zhou, Qingrong Yao

School of Material Science and Engineering, Guilin University of Electronic Technology, Guangxi, Guilin, 541004, PR China

ARTICLE INFO

Article history:
Received 6 October 2015
Received in revised form
17 November 2015
Accepted 19 November 2015
Available online 23 November 2015

Keywords:
$NaMgH_3$
Perovskite structure
Decomposition
Dehydriding kinetic property
Ball milling

ABSTRACT

$NaMgH_3$ hydride with perovskite structure has been synthesized by high-energy ball milling, the maximum hydrogen-desorbed amount of which is 3.42 wt.% at 638 K. Two decomposition steps have been detected for perovskite-type $NaMgH_3$ hydride, calculated values of activation energy for the two steps are 180.25 ± 8.25 kJ/mol and 156.23 ± 18.54 kJ/mol by Kissinger method. In comparison with $NaMgH_3$ hydride, $Li_{0.5}Na_{0.5}MgH_3$ hydride has better dehydriding kinetic properties and higher hydrogen-desorbed amount (4.11 wt.%) due to partial replacement of Na by Li. $LiMgH_3$ hydride with perovskite structure cannot be synthesized by milling of the mixture of LiH and MgH_2 hydrides. However, the maximum hydrogen-desorbed amount of this milled mixture is 5.54 wt.% at 638 K, this may suggest that LiH is a good catalyst for dehydrogenation of MgH_2, but further research is needed.

1. Introduction

Hydrogen has great potential as an efficient fuel and is a good energy carrier, especially in the terms of energy sustainability and environmental conservation. However, it's large-scale use for mobile applications is still limited by storage issues. Hydrogen storage in the solid state is currently considered as the best option for a safe and long-term solution [1–10]. Recently, Mg-based perovskite-type hydrides, $AMgH_3$ (A = alkali-earth element), have received considerable attention [11–16].

$NaMgH_3$ was studied as a potential candidate for on-board applications because it has high gravimetric and volumetric densities (6 wt.% and 88 kg/m^3) as well as reversible hydriding and dehydriding reactions [14]. Also, it was pointed out as a potential material for future generation of electronic devices due to the superior hydrogen mobility of the perovskite structure [11]. $NaMgH_3$ [17] has an orthorhombic perovskite structure analogous to the $GdFeO_3$ type (space group Pnma) which is common in low tolerance factor oxide perovskites, where the singly charged Na cation occupies eight-fold coordinated voids. *Sheppard* et al. measured the kinetic and thermodynamic data for the decomposition of $NaMgH_3$ into NaH and Mg. The desorption enthalpy and entropy are 86.6 ± 1.0 kJ/(mol H_2) and 132.2 ± 1.3 kJ/(mol H_2 K) respectively, indicating that $NaMgH_3$ is thermodynamically more stable than MgH_2 [18].

It is shown that the thermodynamic properties of $NaMgH_3$ can be tuned by incorporating new elements or doping catalytic additives [19,20]. For example, the hydrogen storage properties of $NaMgH_3$ in situ embedded of Mg_2NiH_4 and YH_3 nanoparticles was studied by *Li's group* and they found that the composite material exhibited greatly enhanced kinetics for hydrogen absorption and desorption cycling after doping [10]. Moreover the onset temperature of decomposition was successfully decreased with the additions of Si element doped into $NaMgH_3$ by mechanical milling as reported by *Anna-Lisa Chaudhary* and co-workers [20]. *Martínez-Coronado* et al. [21] prepared $Na_{1-x}Li_xMgH_3$ (X = 0, 0.25, 0.5) ternary hydrides using a high-pressure technique, and found that as Li is introduced in the system, the unit-cell parameters decrease, the tilting angle increases and the MgH_6 octahedra become more distorted due to the smaller ionic size of Li^+ vs Na^+. The hydrogen desorption temperature decreases due to the lower structural stability of the Li-containing perovskites. *Xiao* et al. [22] also predicted the same results based on density functional theory calculations.

The replacement of Na by Li would be advantageous for the hydrogen storage ability of $NaMgH_3$ hydrides [23,24] due to the following reasons: (i) Li is lighter than Na, so the amount of hydrogen per hydride mass should be improved and (ii) the stability of Li perovskite is found to be lower, therefore the hydrogen

* Corresponding author.
E-mail address: ghab1987@163.com (Z.-m. Wang).

http://dx.doi.org/10.1016/j.jallcom.2015.11.127
0925-8388/

desorption proceeds at lower temperatures. In this work, high-energy ball-milling under H_2, is employed to prepared $Na_{1-x}Li_xMgH_3$ (x = 0, 0.5, 1.0) hydrides, a comprehensive study of the phase structure before/after heat-treatment, thermal analysis and hydrogen-desorbed amount and dehydriding kinetic properties have been investigated.

2. Experimental procedure

Nominal composition $Na_{1-x}Li_xMgH_3$ (x = 0, 0.5, 1.0) samples, were prepared from stoichiometric mixtures of MgH_2 (>98% purity, Alfa-Aesar), NaH and LiH (>95% Purity, Sigma-Aldrich). The mixed powders were milled with stainless steel balls under H_2 atmosphere (0.8 MPa) for 45 h at 320 rpm using a YXQM-2l planetary mill at the ambient temperature. The weight ratio of ball to powder is 80:1. Partial as-milled samples were selected and heat-treated for 5 h under H_2 atmosphere (3 MPa) at 623 K, then cooled to room temperature for structure analysis and dehydriding test.

X-ray diffraction (XRD) analysis of samples were performed on Empyrean PIXcel 3D (Cu Ka radiation) diffractometer. The powder samples were sealed in a special cell, coated with Kapton film to prevent exposure to air. The evaluation of hydrogen-desorbed amount and dehydriding kinetic properties of samples were measured on automatic Sievert-type apparatus (PCTpro2000, Setaram Co.). Thermostability properties of as-milled samples were investigated by DSC analysis (DSC, NETZSCH STA 449F3) at different heating rates (5, 10, 15 K/min) under a continuous argon flow (20 ml/min) from 298 K to 725 K, and testing samples were sealed with aluminum metal crucible. All sample handlings were undertaken in an argon atmosphere glovebox (Mbraun, Labstar, 1 ppm H_2O, 1 ppm O_2).

3. Results and discussion

3.1. Synthesis, dehydriding properties and thermal analysis of $NaMgH_3$ hydrides

Fig. 1 displayed the XRD patterns of as-milled $NaMgH_3$ samples before/after heat-treatment. The peaks of $NaMgH_3$ phase can be observed in as-milled sample, which is an orthorhombic perovskite structure, similar to the $GdFeO_3$ type (space group Pnma) [25,26]. More sharp peaks of $NaMgH_3$ phase can be seen in the sample after heat-treatment, accompanied with the peaks of MgH_2 and NaH phases. This results indicate that the crystallinity of $NaMgH_3$ sample can be improved by heat-treatment at 623 K for 5 h (H_2, 3 MPa). There are MgH_2 and NaH phases after heat treatment. This is why we think maybe heat treatment can make MgH_2 and NaH phases which are unreactive and have a broken crystal structure to form new crystals. The existence of MgO phase can be attributed to the slight oxidization of samples in the handling process [27].

Fig. 2 shows the isothermal dehydriding properties of as-milled $NaMgH_3$ samples at 638 K, and the hydrogen-desorption pressure is 10^{-2} bar. As illustrated in Fig. 2, dehydriding kinetics of as-milled $NaMgH_3$ hydride without heat-treatment is superior to that after heat-treatment, the maximum hydrogen-desorbed amount of the former is 3.42 wt.%, which will release above 3 wt.% of the amount within 40 min. However, the dehydriding process of the latter is quite slow with hydrogen-desorbed amount less than 3 wt.% after 170 min. Possible reasons may be: (1) Partial decomposition of $NaMgH_3$ perovskite hydride will occur in the heat-treated process, the products is MgH_2 and NaH hydrides, the dehydriding temperatures of the two products are higher than that of $NaMgH_3$ hydride [27–29], so results in the decrease of the total hydrogen-desorbed amount of as-milled $NaMgH_3$ hydride. (2) As-milled sample possesses some amorphous structure, more defects and large grain boundaries which will lead to the improvement of dehydriding kinetic properties, but such structure feature will greatly be disappeared after heat-treated process. In other word, the heat-treatment will increase the crystallinity of the sample, but reduce its dehydriding kinetic properties. The hydrogen-desorbed amounts of the sample before/after heat-treatment are also listed in Table 1.

Fig. 3 shows the isothermal dehydriding properties of as-milled $NaMgH_3$ hydride at different temperature, and the hydrogen-desorbed amounts are also listed in Table 1. As can been seen, the hydrogen-desorption rate accelerated with increasing temperature. The maximum hydrogen-desorbed amount of $NaMgH_3$ sample is 3.42 wt.%, and about 90% of the amount is released within 47 min at 638 K, but the hydrogen-desorbed amount is 2.03 wt.% at 613 K, and only 1.13 wt.% (after 150 min) at 593 K.

The XRD patterns of $NaMgH_3$ samples after dehydriding at different temperature are shown in Fig. 4. As can been seen, peaks of $NaMgH_3$ phase are still in existence, and peaks of NaH phase and Mg phase can also be observed. With the increase of temperature from 593 K to 638 K, peaks of $NaMgH_3$ phase become weakened, and peaks of NaH phase and Mg phase become strengthened. The

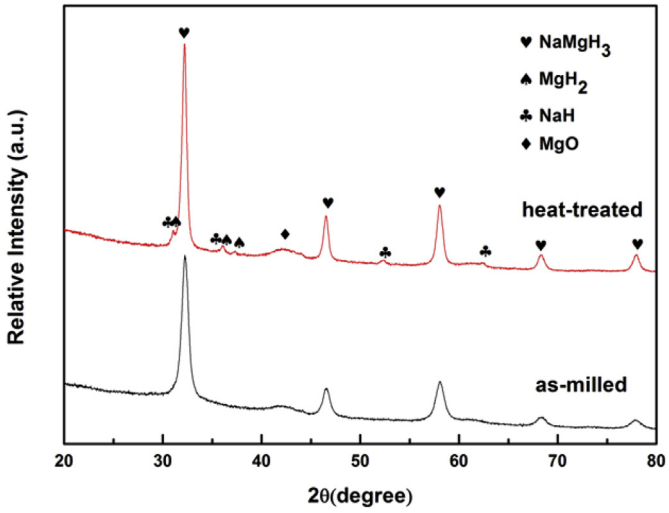

Fig. 1. XRD patterns of as-milled $NaMgH_3$ hydrides before/after heat-treatment.

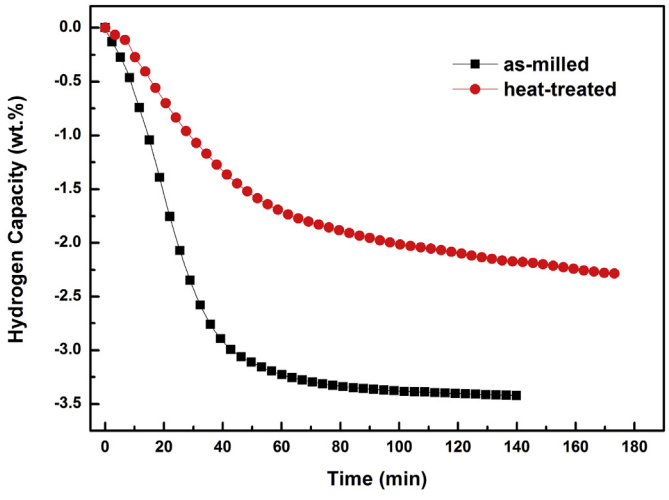

Fig. 2. Dehydriding kinetic curves of as-milled $NaMgH_3$sample before/after heat-treatment at 638 K.

Table 1
The hydrogen-desorbed amounts of $NaMgH_3$ sample before/after heat-treatment.

Method	593 K	613 K	638 K
As-milled	1.13 wt.%	2.03 wt.%	3.42 wt.%
Heat-treated	/	/	2.28 wt.%

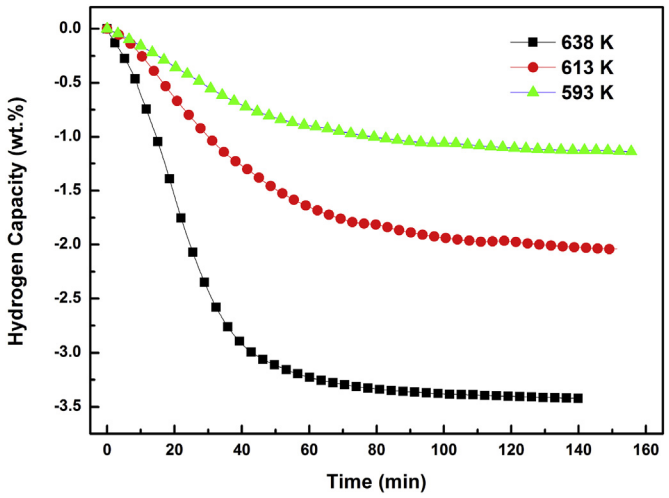

Fig. 3. Dehydriding kinetic curves of as-milled $NaMgH_3$ hydride at different temperature.

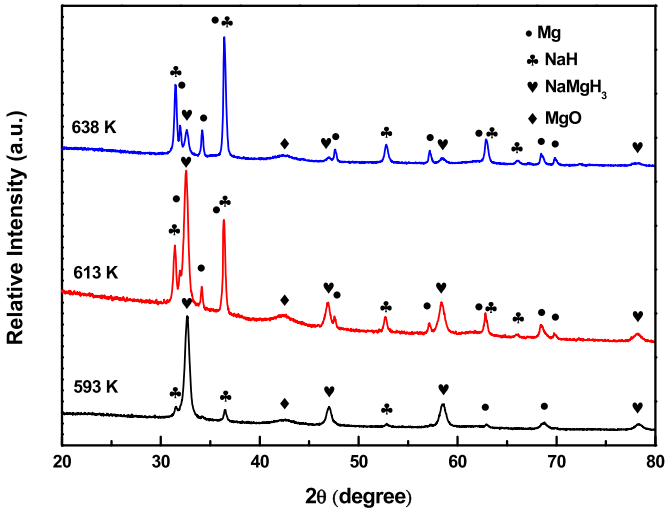

Fig. 4. XRD patterns of as-milled $NaMgH_3$ hydride after dehydriding at different temperature.

result indicates that the decomposition of $NaMgH_3$ hydride will occurred in the dehydriding process and the decomposition products are MgH_2, NaH and H_2. The decomposed H_2 will contribute to the hydrogen-desorbed amount of the sample, but this decomposition is not fully finished at this condition.

Fig. 5 shows the DSC curves of as-milled $NaMgH_3$ hydride at different heating rates (5, 10, 20 K/min) under a continuous argon flow from 298 to 750 K. Herein Tx and Tp stand for the start and peak temperature of dehydrogenation, respectively. We observed that there are two dehydriding processes, Tx and Tp rise clearly with increased heating rate and these data are listed in Table 2. According to results of Figs. 4 and 5, the following dehydrogenation steps can be deduced:

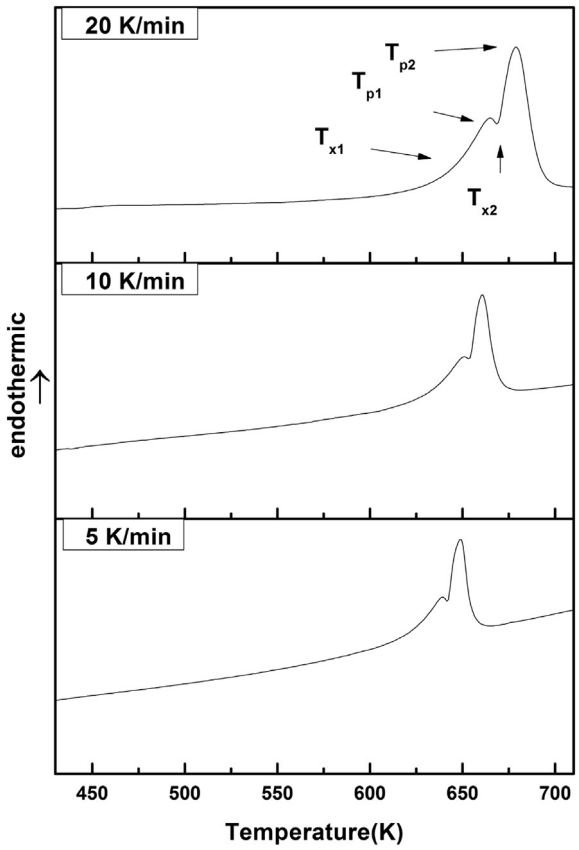

Fig. 5. DSC curves of as-milled $NaMgH_3$ hydride at different heating rate.

Table 2
Dehydriding temperatures of $NaMgH_3$ hydride at different heating rate.

Rate	T_{x1}	T_{p1}	T_{x2}	T_{p2}
5 K/min	623.3 K	639.4 K	642.6 K	649.0 K
10 K/min	632.8 K	651.0 K	654.6 K	660.8 K
20 K/min	639.3 K	665.0 K	669.9 K	679.0 K
ΔE	180.25 ± 8.25 kJ/mol		156.23 ± 18.54 kJ/mol	

$$NaMgH_3 \rightarrow NaH + Mg + H_2 \quad (1)$$

$$NaH \rightarrow Na + 1/2H_2\uparrow \quad (2)$$

This explanation agrees well with the previous works [19,20]. Based on the two decomposition steps of $NaMgH_3$ hydride, the theoretical hydrogen-desorbed amount of the first step is 4 wt.%, and 2 wt.% for the second step. In this work, the experimental data is 3.42 wt.% at 638 K, which is about 85.5% of the theoretical hydrogen-desorbed amount of the first step. The second step was not carried out due to the limitation of working temperature of PCI apparatus.

In order to estimate the activation energy (ΔE) for dehydrogenation of the as-milled $NaMgH_3$ hydride, the Kissinger relation is frequently used for non-isothermal DSC analysis, and can be expressed in the form as [30].

$$\ln (Tp^2/\upsilon) = \Delta E/RT + \ln (\Delta E/Ru_0). \quad (3)$$

where R is the gas constant, and υ and u_0 are heating rate and frequency factor respectively. Fitting curves by Kissinger method are shown in Fig. 6, which represent a good linear relation between

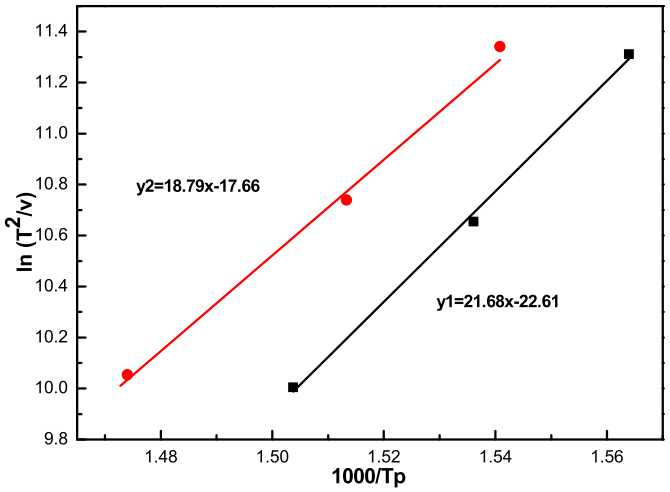

Fig. 6. The relationships between ln (Tp2/v) and (1000/Tp) for $NaMgH_3$ hydride fitted by Kissinger method.

ln (Tp^2/υ) and ($1000/T_p$) with a slope of $\Delta E/R$. It can be found that ΔE_1 for the first decomposition step of as-milled $NaMgH_3$ hydride is 180.25 kJ/mol, and 156.23 kJ/mol (ΔE_2) for the second step. Where measured $NaMgH_3$ sample was synthesized by a two-step method (consisting of ball milling and hydriding combustion synthesis). This work suggests that as-milled $NaMgH_3$ hydride has better dehydriding property.

3.2. Structure and dehydriding properties of $Li_xNa_{1-x}MgH_3$ hydrides

The XRD patterns of nominal composition $Li_xNa_{1-x}MgH_3$(x = 0, 0.5, 1.0) samples are shown in Fig. 7. The following points can be deduced from Fig. 7, (1) In the case of x = 1.0, peaks of unreacted LiH and MgH_2 are detected, no new phase can be formed indicating that $LiMgH_3$ hydride cannot be synthesized by mechanical ball-milling of the mixture of LiH and MgH_2 hydrides. (2) In the case of x = 0.5, Peaks of $NaMgH_3$ and MgH_2 phases have been observed, LiH is not observed, probably because the latter is eventually present as an amorphous phase after ball-milling [21]. (3) In $Li_{0.5}Na_{0.5}MgH_3$ sample, peaks of $NaMgH_3$ phase shift to higher diffraction angles as Na atoms are replaced by Li. This is due to the smaller size of the Li cations.

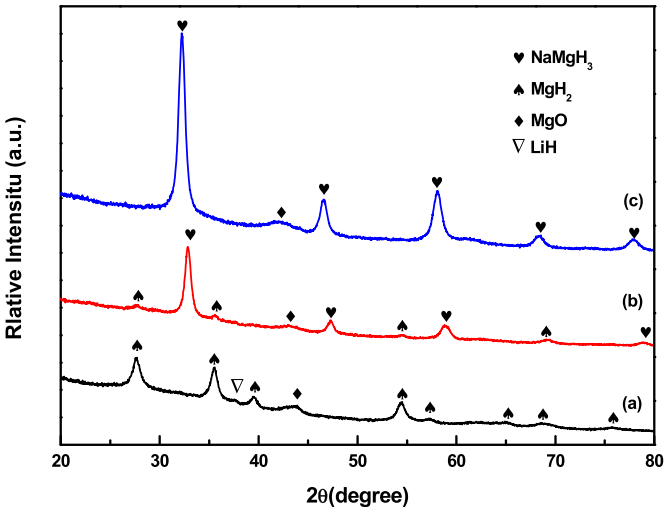

Fig. 7. The XRD patterns of nominal composition $Li_xNa_{1-x}MgH_3$ samples (a) x = 1(b) x = 0.5(c) x = 0.

In addition, tolerance factor (t) can be used to predict structure stability of ABX_3 perovskite-type compound. When H is X, the equation is expressed as follow:

$$t = (R_A + R_H)\Big/\sqrt{2}(R_B + R_H) \quad (4)$$

Here R_A and R_B stand for cationic Ionic radius of A and B respectively, R_H is hydrogen anion radius. Electronic distribution of H is not spherical-scattering type in hydride pattern, R_H is not fixed, and the covalent bond length varied with different cationic ions. The calculation of tolerance factor (t) is based on the fixed ion radius, so R_H is set as 0.140 nm [26,31]. No accurate tolerance factor range for perovskite-type hydrides is given at present. However, by analogy with perovskite-type oxides and halides, *Ikeda* et al. reported that a reasonable range of tolerance factor is 0.77 < t < 1.00, and perovskite-type hydride with stable structure are suggested to be existent within this range [32]. The calculated tolerance factor (t) are listed in Table 3. The results illustrate that perovskite-type $NaMgH_3$ hydride can be stably existing at t = 0.807, wheres t value of $Li_xNa_{1-x}MgH_3$(x = 0.5) perovskite structures is 0.767 (near 0.77), indicating that partial replacement of Na with Li will reduce the tolerance factor, and form distorted perovskite structure. $LiMgH_3$ perovskite hydride cannot be formed for t = 0.727. In fact, $LiMgH_3$ ternary hydride has not been successfully synthesized so far. Vajeeston et al. reported that $LiMgH_3$ is a stable trigonal structure of $LiTaO_3$ via first-principles prediction [33].

The replacement of Na by Li would be advantageous for the hydrogen storage ability of the parent material [23,24] since (i) Li is lighter than Na, so the amount of hydrogen per hydride mass should be improved and (ii) the stability of the Li perovskite is found to be lower, therefore the hydrogen desorption proceeds at lower temperatures. Fig. 8 shows dehydriding kinetic curves of $Li_xNa_{1-x}MgH_3$ hydrides at 638 K. The maximum hydrogen-desorbed amount increases with the increase of x, In comparison with $NaMgH_3$ hydride, $Li_{0.5}Na_{0.5}MgH_3$ hydride has better dehydriding kinetic properties, and released about 90% of the maximum hydrogen-desorbed amount within 28 min, which is possibly due to the formation of distorted perovskite structure caused by partial replacement of Na by Li. However, $Li_xNa_{1-x}MgH_3$(x = 1.0) can be regard as a ball-milled mixture of LiH and MgH_2 hydrides, which has 5.54 wt. % of the maximum hydrogen-desorbed amount, and releases about 90% of the maximum hydrogen-desorbed amount within 23 min at 638 K further indicating that LiH has good catalytic effect for dehydriding properties of MgH_2 in this milling condition.

Measured and theoretical hydrogen-desorbed amounts of nominal composition $Li_xNa_{1-x}MgH_3$ hydrides are listed in Table 3. The theoretical value is related to the first decomposition step of $NaMgH_3$ hydride. The hydrogen-desorbed amount increases according to x = 1.0 > x = 0.5 > x = 0, which suggest Li doping is beneficial for dehydriding properties of Li—Na—Mg—H system hydrides. In fact, based on density functional theory calculation, *Xiao's group* [22] found that the dehydrogenation enthalpy of perovskite-

Table 3
Calculated tolerance factor (t) of $Li_xNa_{1-x}MgH_3$ samples.

Sample	x = 0	x = 0.5	x = 1.0
t	0.807	0.767	0.727
Desorp. H_2 (wt. %)	3.42	4.11	5.54
Theoretical H_2 (wt. %)	4.01	4.77	5.88
Percentage (%)	85.5	86.2	94.2

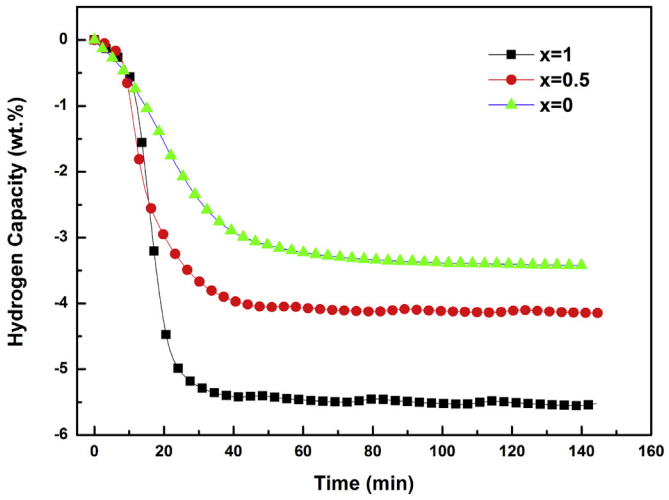

Fig. 8. Dehydriding kinetic curves of nominal composition $Li_xNa_{1-x}MgH_3$(x = 0, 0.5, 1.0) samples at 638 K.

type $NaMgH_3$ hydride can be reduced by the replacement of Na by Li, thereby enhance its dehydriding properties. Our results are consistent with this theoretical prediction.

4. Conclusions

1) $NaMgH_3$ hydride with perovskite structure has been synthesized by high-energy ball milling and the maximum hydrogen-desorbed amount is 3.42 wt. % at 638 K. The crystallinity of as-milled $NaMgH_3$ will be improved by above-adopted heat-treatment, but its dehydriding properties will be reduced obviously.
2) Two decomposition steps have been detected for perovskite-type $NaMgH_3$ hydride. Based on Kissinger method, calculated values of activation energy for the two steps are 180.25 ± 8.25 kJ/mol (ΔE_1) and 156.23 ± 18.54 kJ/mol (ΔE_2) respectively.
3) In comparison with $NaMgH_3$ hydride, $Li_{0.5}Na_{0.5}MgH_3$ hydride has better dehydriding kinetic properties and higher hydrogen-desorbed amount (4.11 wt.%) due to partial replacement of Na by Li, which can release about 90% of the maximum hydrogen-desorbed amount within 28 min.
4) $LiMgH_3$ hydride with perovskite structure cannot be synthesized with the mixture of LiH and MgH_2 hydrides. However, the maximum hydrogen-desorbed amount of this ball-milled mixture is 5.54 wt.% at 638 K, indicating LiH is a good catalyst for dehydrogenation of MgH_2.

Acknowledgments

This work was financially supported by the National Natural Science Foundation of China (No. 51261003, 51471055, 51371061 and 21363005) and Guangxi Experiment Center of Information Science, Guilin University of Electronic Technology (20130113).

References

[1] M. Bououdina, D. Grant, G. Walker, Int. J. Hydrogen Energy 31 (2006) 177–182.
[2] Z. Cao, L. Ouyang, Y. Wu, et al., Dual-tuning effects of In, Al, and Ti on the thermodynamics and kinetics of $Mg_{85}In_5Al_5Ti_5$ alloy synthesized by plasma milling, J. Alloys Compd. 623 (2015) 354–358.
[3] Y. Yang, Y. Liu, Y. Zhang, et al., Hydrogen storage properties and mechanisms of $Mg(BH_4)_2{\cdot}2NH_{3-x}MgH_2$ combination systems, J. Alloys Compd. 585 (2014) 674–680.
[4] M. Wang, X. Li, M. Gao, et al., A Novel synthesis of MgS and its application as electrode material for lithium-ion batteries, J. Alloys Compd. 603 (2014) 158–166.
[5] Z.J. Cao, L.Z. Ouyang, H. Wang, et al., Structural characteristics and hydrogen storage properties of Sm_2Co_7, J. Alloys Compd. 608 (2014) 14–18.
[6] Z. Cao, L. Ouyang, H. Wang, et al., Composition design of Ti–Cr–Mn–Fe alloys for hybrid high-pressure metal hydride tanks, J. Alloys Compd. 639 (2015) 452–457.
[7] D. Wu, L. Ouyang, C. Wu, et al., Phase transition and hydrogen storage properties of Mg–Ga alloy, J. Alloys Compd. 642 (2015) 180–184.
[8] L.Z. Ouyang, Z.J. Cao, H. Wang, et al., Enhanced dehydriding thermodynamics and kinetics in Mg(In)-MgF_2 composite directly synthesized by plasma milling, J. Alloys Compd. 586 (2014) 113–117.
[9] L.Z. Ouyang, X.S. Yang, M. Zhu, et al., Enhanced hydrogen storage kinetics and stability by synergistic effects of in situ formed $CeH_{2.73}$ and Ni in $CeH_{2.73}$-MgH_2-Ni nanocomposites, J. Phys. Chem. C 118 (2014) 7808–7820.
[10] L.Z. Ouyang, J.J. Tang, Y.J. Zhao, et al., Express penetration of hydrogen on Mg(1013) along the close-packed-planes, Sci. Rep. 5 (2015) 10776.
[11] D. Pottmaier, E.R. Pinatel, J.G. Vitillo, S. Garroni, M. Orlova, M.D. Baro, Structure and thermodynamic properties of the NaMgH3 perovskite: a comprehensive study, Chem. Mater. 23 (2011) 2317–2326.
[12] Y. Bouhadda, N. Fenineche, Y. Boudouma, Hydrogen storage: lattice dynamics of orthorhombic $NaMgH_3$, Phys. B 406 (2011) 1000–1003.
[13] P. Vajeeston, P. Ravindran, A. Kjekshus, H. Fjellvag, First-principles investigations of the $MMgH_3$ (M=Li, Na, K, Rb, Cs) series, J. Alloys Compd. 450 (2008) 327–337.
[14] Y. Bouhadda, Y. Boudouma, N. Fenineche, A. Bentabet, Ab initio calculations study of the electronic, optical and thermodynamic properties of $NaMgH_3$, for hydrogen storage, J. Phys. Chem. Solids 71 (2010) 1264–1268.
[15] H. Wu, W. Zhou, T.J. Udovic, J.J. Rush, T. Yildirim, Crystal chemistry of perovskite-type hydride $NaMgH_3$: implications for hydrogen storage, Chem. Mater. 20 (6) (2008) 2335–2342.
[16] Y. Bouhadda, M. Bououdina, N. Fenineche, Y. Boudouma, Elastic properties of perovskite-type hydride $NaMgH_3$ for hydrogen storage, Int. J. Hydrogen Energy 38 (2013) 1484–1489.
[17] A. Bouamrane, J.P. Laval, J.P. Soulie, J.P. Bastide, Structural characterization of $NaMgH_2F$ and $NaMgH_3$, Mater. Res. Bull. 35 (2000) 545–549.
[18] D.A. Sheppard, M. Paskevicius, C.E. Buckley, Thermodynamics of hydrogen desorption from $NaMgH_3$ and its application as a solar heat storage medium, Chem. Mater. 23 (2011) 4298–4300.
[19] Y. Li, L. Zhang, Q. Zhang, F. Fang, D. Sun, K. Li, H. Wang, L. Ouyang, M. Zhu, In situ embedding of Mg_2NiH_4 and YH_3 nanoparticles into bimetallic hydride $NaMgH_3$ to inhibit phase segregation for enhanced hydrogen storage, J. Phys. Chem. C 118 (14) (2014) 23635–23644.
[20] A. Chaudhary, M. Paskevicius, D.A. Sheppard, C.E. Buckley, Thermodynamic destabilisation of MgH_2 and $NaMgH_3$ using Group IV elements Si, Ge or Sn, J. Alloys Compd. 623 (2015) 109–116.
[21] R. Martínez-Coronado, J. Sánchez-Benítez, M. Retuerto, M.T. Fernández-Díaz, J.A. Alonso, High-pressure synthesis of $Na_{1-x}LixMgH_3$ perovskite hydrides, J. Alloys Compd. 522 (2012) 101–105.
[22] X.-B. Xiao, B.-Y. Tang, S.-Q. Liao, L.M. Peng, W. Ding, Thermodynamic and electronic properties of quaternary hydrides $Li_xNa_{1-x}MgH_3$, J. Alloys Compd. 474 (2009) 522–526.
[23] K. Ikeda, Y. Nakamori, S. Orimo, Formation ability of the perovskite-type structure in $Li_xNa_{1-x}MgH_3$ (x=0, 0.5 and 1.0), Acta Mater. 53 (2005) 3453–3457.
[24] K. Ikeda, Y. Kogure, Y. Nakamori, S. Orimo, Formation region and hydrogen storage abilities of perovskite-type hydrides, Solid State Chem. 35 (2007) 329–337.
[25] E. RÖnnebro, D. Noréus, K. Kadir, A. Reiser, B. Bogdanovic, Investigation of the perovskite related structures of $NaMgH_3$, $NaMgF_3$ and Na_3AlH_6, J. Alloys Compd. 299 (2000) 101–106.
[26] A. Bouamranea, J.P. Laval, J.-P. Soulie, J.P. Bastide, Structural characterization of $NaMgH_2F$ and $NaMgH_3$, Mater. Res. Bull. 35 (2000) 545–549.
[27] H. Reardon, N. Mazur, D.H. Gregory, Prog. Nat. Sci. Mater. 23 (3) (2013) 343–350.
[28] K. Ikeda, Y. Kogure, Y. Nakamori, S. Orimo, Scr. Mater. 53 (2005) 319–322.
[29] D. Pottmaier, E.R. Pinatel, J.G. Vitillo, S. Garroni, M. Orlova, et al., Chem. Mater. 23 (2011) 2317–2326.
[30] H.E. Kissinger, Anal. Chem. 29 (1957) 1702–1706.
[31] G.G. Libowitz, The Solid-state Chemistry of Binary Metal Hydrides, WA Benjamin, 1965.
[32] H. Wang, J. Zhang, J.W. Liu, L.Z. Ouyang, M. Zhu, J. Alloys Compd. 580 (2013) 197–201.
[33] P. Vajeeston, P. Ravindran, A. Kjekshus, H. Fjellvåg, J. Alloys Compd. 450 (2008) 327–337.